CORE
Metadata, citation and similar papers at core.ac.uk
Provided by NASA Technical Reports Server

THE EFFECTS OF NEWLY MEASURED CROSS SECTIONS IN HYDROGEN ON THE PRODUCTION OF SECONDARY NUCLEI DURING THE PROPAGATION OF COSMIC RAYS THROUGH INTERSTELLAR H

W. R. Webber & M. Gupta
Space Science Center
University of New Hampshire
Durham, NH 03824

L. Koch-Miramond & P. Masse
Cen Saclay 91191
Gif-sur-Yvette
Cedex, France

1. Introduction. As discussed in papers at this conference and in earlier publications (e.g. Webber & Brautigam, 1982) we have now measured the cross sections of six important cosmic ray source nuclei in hydrogen at several energies between 300 and 1800 MeV/nuc. Significant differences, sometimes exceeding 50%, exist between these new measurements and the earlier semi-empirical predictions, and we are in the process of determining a new set of semi-empirical formulae that better describe this fragmentation (Webber & Hsiung, paper, OG 7.2-24 this conference). We have now obtained enough new cross sections so that the systematics of their effects on cosmic ray propagation through interstellar hydrogen can be examined.

2. Details of Calculation. In this study we have used the propagation program developed by the HEAO-3 experimenters at SACLAY (e.g. Perron and Koch, 1981) as well as a simpler program developed at UNH. For the purposes of this study, for all calculations, we have assumed a source spectrum ~ $P^{-2.3}$ and an exponential distribution of path lengths, $\lambda_e = 22.0\ \beta\ P^{-0.6}\ g/cm^2$ of hydrogen above 5.5 GV and $\lambda_e =$ = 8.33 β below 5.5 GV. This path length is found to fit a wide variety of cosmic ray abundance data at both high and low energies and for various Z ratios as discussed by Soutoul et al., paper, OG 4.1-3 this conference. No truncation of this path length is considered in these calculations. For the cross sections we have used 1) the earlier semi-empirical formula predictions as updated through 1977 (Tsao and Silberberg, 1979) and 2) revised cross sections as indicated by our new results - including unmeasured cross sections as revised by our updated semi-empirical formulae (Webber and Hsiung, paper, OG 7.2-24 this conference).

3. Results of Calculation. a) Abundance Ratios. In Figures 1, 2 & 3 we show the B/C, A1/Si and K/Fe ratios calculated for secondary production only. (Φ = 600 MV in all cases). The observed ratios (Engelmann et al., 1983) are also shown. In almost every case the new cross sections lead to significantly better fits to the measured individual ratios of mainly secondary nuclei than was the case for the previous semi-empirical cross sections. In order to further illustrate the propagational changes brought about by the new cross sections we examine the situation at one energy only - 1.5GeV/nuc where $\lambda_{esc} = 8.0 g/cm^2$. Table I lists the percentage change in secondary production for the various ratios brought about by introducing the new cross sections. It should be pointed out that these percentage changes are at one energy only. They may differ considerably at other energies because of different energy dependances of the cross sections as illustrated in Figure 3. Also note that these differences, which are typically

5-10% or larger, are much greater than the 1-2% abundance ratio errors in the HEAO data base. And finally, the effects of short path length truncation, which are typically ~ 5-10% in the ratio of B/C to the ratio of Z=21-25/Fe, (for example Garcia-Munoz et al., 1984) can be masked by the differences of the same order found for the new cross sections.

b) Source Abundances. The new cross sections allow the secondary abundances of most nuclei to be caluclated to an accuracy ~ 3-5% for a fixed path length. This, coupled with the 1-2% accuracy of the measured charge ratios, allows the source abundance of galactic cosmic ray nuclei to be calculated to a new level of precision, including some charges for which only upper limits existed from previous calculations. This analysis is shown in Table 2. All values refer to 1.5 GeV/nuc and use the propagation parameters already discussed, e.g. λ_e = 8.0g/cm^2, Φ = 600 MV. The caluclated abundance at earth in column one is the secondary abundance only as caluclated from all heavier nuclei -including the revised source abundance from this work. The errors are only those on the cross sections as propagated through the 8.0g/cm^2 of interstellar hydrogen. The observed ratios are the average ratios at 1.5 GeV/nuc from Engelmann et al., 1983. Any differences in the calculated and observed ratios for the mostly secondary nuclei can be directly related to the source abundance of that secondary nucleus. It is seen that for Be, B, Fl, Cl, K, Sc and V this difference is ~ $\pm$ 1 σ in the combined errors in the cross sections and the observations. The fact that these differences are almost equally divided between + and - and also show no clear trend with Z shows that 1) the value of 8.0g/cm^2 is consistent to within $\pm$ 0.2g/cm^2 and 2) the effects of truncation of short path lengths must be small.

These differences translate into source abundances of a few parts in 1000 to that of Si, with comparable errors. For the remaining nuclei in the table the source abundances are all finite and significant. For the first time it is possible to get meaningful source abundance estimates for the elements P, Ar, Ti and Cr. If the usual plot of the ratio of CRS to LG abundances (≡R_1) versus FIP is made (Figure 4) then a rather abrupt decrease from a value ~ 1 to a value ~ 0.2-0.3 is observed between 8-12V FIP. The elements He, N and Ti and Cr apparently do not fit this simple picture. A very similar behavior occurs when a corresponding plot is made using new and more complete solar particle data from Voyager (Breneman et al., 1985). In Figure 5 we show a plot of the new cosmic ray source data versus the new solar particle abundance data. (≡R_2) Earlier plots of this type suggested ratios R_2 ~ 1 with some notable exceptions. There is now evidence for a structure in this abundance ratio when plotted against FIP. To further examine this we plot in Figure 6 R_1 vs R_2. Seven elements are clustered about one - several of the remaining elements are clustered about R_1 = 0.25 & R_2 = 0.7 suggesting perhaps a difference in the FIP selection process in the sun and in cosmic ray sources for these elements. This selection process or fractionization occurs on the sun between the photosphere and corona and its identification in the cosmic ray sources would be of great importance. It is also possible that all of the elements, except C, lie along a line in R_1 R_2 space as indicated by the line in Figure 6. The further implications of this behavior will be discussed in a separate publication.

4. Acknowledgements. This work was supported by a HEAO Guest Investigator Grant #NAG-8-451, and by a NASA Support Grant #NGR-30-002-052.

5. References.

Breneman, H., et al., paper SP this conference
Engelmann, J. J., et al., *17thICRC*, **2**, 17, 1983
Garcia-Munoz, M., et al., *Ap.J.*, **280**, L13, 1984
Perron, C., & Koch, L., *Proc. 17th ICRC*, **2**, 27, 81
Soutoul, A., et al., paper OG 4.1-3, this conference

Tsao, C. H., &Silberberg, R., *Proc. 16thICRC*, **2**, 202, 1979
Webber, W. R., & Brautigam, D. A., *Ap.J.*, **260**, 894, 1982
Webber, W. R., & Hsiung, P., paper OG 7.2-24, this conference

6. Figure Captions.

Figure 1. The observed B/C ratio and that predicted using the new cross sections.
Figure 2. The observed Al/Si ratio and that predicted using the new cross sections. (Secondary production only - no Al in source)
Figure 3. The observed K/Fe ratio and that predicted using the new cross sections - no K in source.
Figure 4. Ratio of cosmic ray source abundance deduced in this analysis to LG abundances vs FIP $\equiv R_1$.
Figure 5. Ratio of new cosmic ray source abundances to new solar cosmic ray abundances vs FIP $\equiv R_2$.
Figure 6. The Ratio R_1 vs. R_2 for elements with $Z \leq 30$.

Table I

Effects of New Cross Sections on Secondary Production Ratios

Ratio	% Change in Secondary Production at 1.5 GeV/nuc*
Be/C	- 3.5
B/C	- 7.3
N/O	+ 5.2
Fl/Ne	≤ 2
Na/Mg	≤ 2
Al/Si	+ 17.0
P/S	+ 10.4
Cl/Fe	- 12.5
Ar/Fe	+ 11.5
K/Fe	- 8.5
Ca/Fe	- 6.1
Sc/Fe	+ 3.0
Ti/Fe	+ 3.2
V/Fe	+ 2.5
Cr/Fe	- 10.2
Mn/Fe	- 16.5
	at 600 MeV/nuc
^{25}Mg	+ 11.5
^{26}Mg	+ 33.0
^{29}Si	
^{30}Si	

* From Tsao & Silberberg, 1977

Table II

Comparison of Calculated & Observed Abundances at 1.5 GeV/nuc - Source Abundances

	Calculated	Observed	Difference	Source Abundance Si = 1000
Be/C	0.109±0.004	0.100±0.005	-0.009±0.007	-8±8
B/C	0.295±0.010	0.305±0.006	0.010±0.012	42±50
C/Si	-	6.76 ±0.12	-	4310±100
N/O	0.303±0.008	0.303±0.003	0.043±0.009	220±50
O/Si	-	6.38 ±0.10	-	4960±80
Fl/Ne	0.133±0.003	0.135±0.003	0.002±0.004	1.3±2.5
Ne/Si	-	1.031±0.010	-	615±15
Na/Mg	0.112±0.010	0.174±0.005	0.062±0.011	66±12
Mg/Si	-	1.305±0.010	-	1075±12
Al/Si	0.158±0.007	0.232±0.005	0.074±0.009	76±9
Si	-	-	-	1000
P/S	0.193±0.009	0.225±0.006	0.033±0.011	45±1.5
S/Si	-	0.203±0.004	-	132±6
Cl/Fe	0.079±0.004	0.076±0.002	-0.003±0.005	-2±5
Ar/Fe	0.110±0.004	0.136±0.003	0.026±0.005	18±5
K/Fe	0.095±0.003	0.099±0.002	0.004±0.004	3±3
Ca/Fe	0.118±0.004	0.220±0.004	0.102±0.006	72±6
Sc/Fe	0.053±0.003	0.051±0.002	-0.002±0.004	-2±4
Ti/Fe	0.140±0.003	0.147±0.003	0.007±0.003	6±3
V/Fe	0.069±0.002	0.073±0.002	0.004±0.003	3±3
Cr/Fe	0.110±0.003	0.146±0.003	0.036±0.005	32±5
Mn/Fe	0.090±0.002	0.097±0.002	0.007±0.0025	6±2.5
Fe/Si	-	0.636±0.013	-	915±15
Co/Ni	0.070±0.007	0.128±0.008	0.058±0.011	2.5±0.5
Ni/Si		0.029±0.0015		45±3

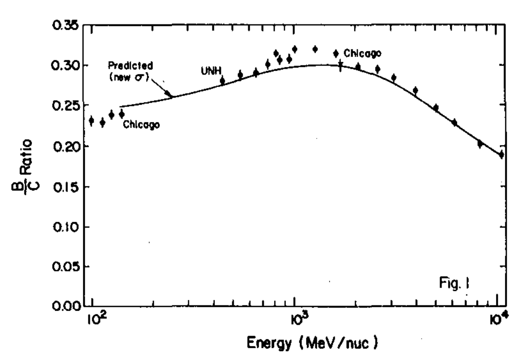

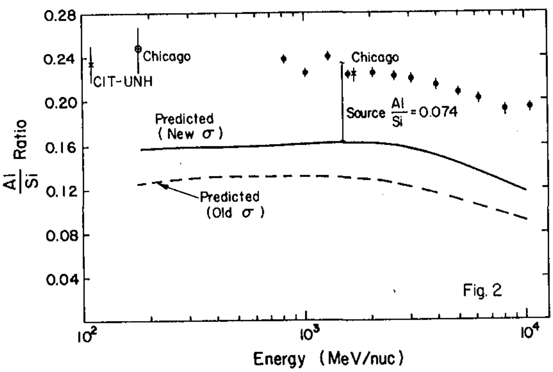
Chicago
CIT-UNH
Chicago
Source Al/Si = 0.074
Predicted (New σ)
Predicted (Old σ)
Al/Si Ratio
Energy (MeV/nuc)
Fig. 2

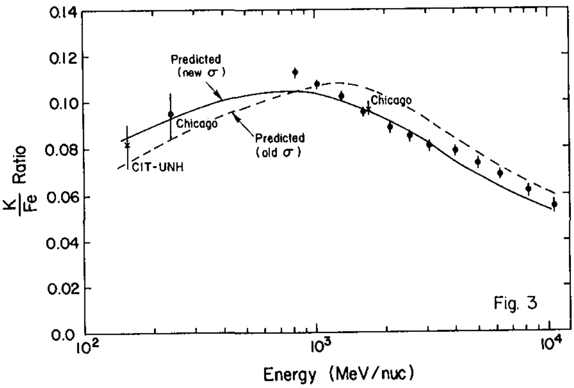
Predicted (new σ)
Chicago
Chicago
Predicted (old σ)
CIT-UNH
K/Fe Ratio
Energy (MeV/nuc)
Fig. 3

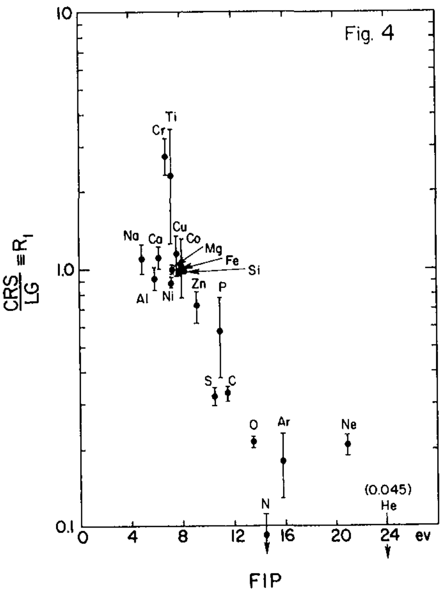
Fig. 4
CRS/LG ≡ R1
FIP
(0.045)
He
ev

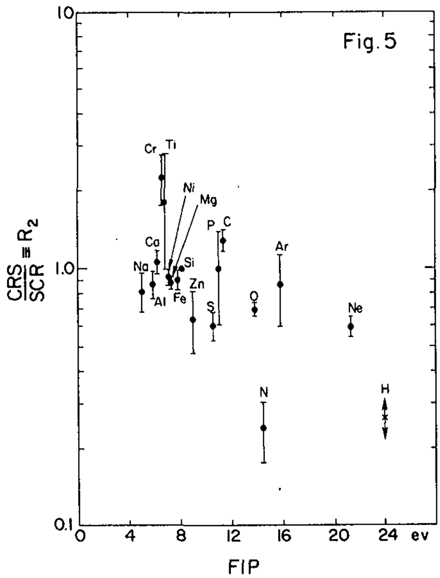
Fig. 5
CRS/SCR ≡ R2
FIP
ev

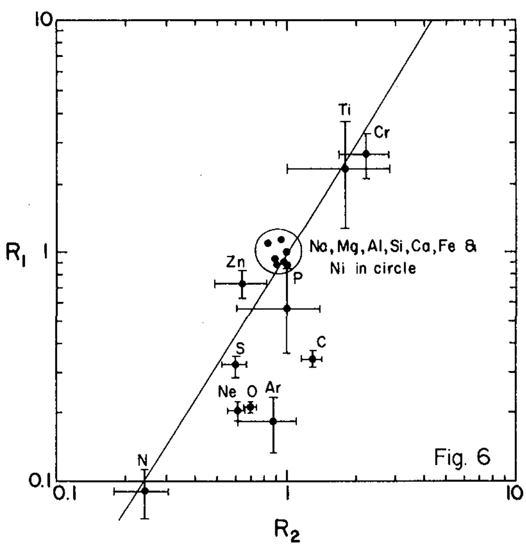
Na, Mg, Al, Si, Ca, Fe & Ni in circle
R1
R2
Fig. 6